Proceedings of the 7th International Conference on HydroScience and Engineering

Philadelphia, USA September 10-13, 2006 (ICHE 2006)

ISBN: 0977447405

Drexel University

College of Engineering

NUMERICAL METHOD TO IMPOSE FREE-SURFACE BOUNDARY CONDITIONS FOR LOCAL FREE-SURFACE FLOWS

Ayumi Saruwatari[1] and Yasunori Watanabe[2]

ABSTRACT

This paper proposes a simple numerical technique to impose free-surface boundary conditions (FSBC) for free-surface flows governed by surface-vortex interactions. Accuracy and efficiency of this technique are examined through the analytical and experimental comparisons. The deformations of a free-surface and evolution of vortices at droplet impacts onto a water pool is reasonably reproduced by properly prescribing FSBC via the proposed method. Typical vortex rings are found to be initiated at the contacts between the droplet and receiving water-surface and to three-dimensionally develop through a splashing process for interacting with a free-surface. The dependencies of flow field on an impact angle of the droplet are also discussed in this study.

1. INTRODUCTION

Breaking waves produce numbers of vortices at wide ranging scales through a splashing process of jets in a surf zone. Although major fluid motion under breaking waves is driven by the large-scale roller vortices, local flows may be predominated by small-scale surface deformations and vortex structures underneath the surface via surface-vortex interactions. While there have been some computational investigations for the dynamic splash-up process and resulting large-scale vortices in breaking waves (e.g. Watanabe & Saeki 1999, Watanabe et al. 2005), local vortices induced within a curved surface boundary layer and local surface deformations due to capillary effects, which is also an important factor to describe wave breaking process, have not been understood. The final goal of this study is to develop a numerical model to describe wave breaking flows involving small- to large-scale turbulence and three-dimensional surface deformations. This study presents a numerical technique to compute local free-surface flows and sub-surface vorticity field governed by the surface-vortex interactions.

There have been some studies dealing with the interaction between a surface and sub-surface vortex. The vorticity is generated on a curved surface where tangential shear must be vanished (Longuet-Higgins 1992). When there is a horizontally located vortex beneath a surface, the surface is involved in the rotating motion and is entrained into an inner fluid region, resulting in a local surface deformation so-called "scar" (Sarpkaya 1996, Brocchini & Peregrine 2001). In order to properly compute the local surface deformation and vorticity field adjacent to the surface via the

[1] Graduate Student, Hydraulic Engineering Laboratory, Hokkaido University, N-13 W-8, Sapporo, Japan (saruwata@eng.hokudai.ac.jp)
[2] Assistant Professor, Hydraulic Engineering Laboratory, Hokkaido University, N-13 W-8, Sapporo, Japan (yasunori@eng.hokudai.ac.jp)

surface-vortex interactions, the dynamic jump conditions must be appropriately given at the surface.

In this study, a numerical technique to satisfy the free-surface boundary conditions (FSBC) in a fixed Cartesian grid system was developed for reproducing the evolving free-surface and vortices produced near the surface under jets.

This paper is organized as follows. The computational method for our large eddy simulation (LES) and proposing technique to impose FSBC are described in section 2, and numerical conditions are explained in section 3. Section 4 presents numerical tests to examine accuracies of our methods. Local vortices and surface deformations under impacting spherical droplet are investigated in section 5. The results are summarized in section 6.

2. COMPUTATIONAL METHOD

Three-dimensional LES for incompressible viscous fluid was performed for the local free-surface flows in the same manner as Watanabe et al. (2005). The following Navier-Stokes equation performed by a filtering operation is used as a governing equation.

$$\frac{D\mathbf{u}}{Dt} = -\frac{1}{\rho}\nabla p + \nu_T \nabla^2 \mathbf{u} + \mathbf{g}, \tag{1}$$

where $\mathbf{u}$ denotes the filtered velocity, p is the pressure, $\mathbf{g}$ is the gravity acceleration and ν_T is the sub-grid viscosity based on the renormarization group theory (Yakhot 1986). All variables are non-dimensionalized by the fluid density ρ, representative length d and velocity v. Equation (1) is split into linear and non-linear finite difference equations on the basis of fractional step method:

$$\frac{\mathbf{u}^{m+\frac{1}{2}} - \mathbf{u}^{m}}{\Delta t} = -\frac{1}{\rho}\nabla p^{m+\frac{1}{2}} + \nu_T \nabla^2 \mathbf{u}^{m+\frac{1}{2}} + \mathbf{g}, \tag{2}$$

$$\frac{\mathbf{u}^{m+1} - \mathbf{u}^{m+\frac{1}{2}}}{\Delta t} + \left[(\mathrm{grad}\,\mathbf{u})\mathbf{u}\right]^{m+\frac{1}{2}} = 0, \tag{3}$$

where m denotes the time step. Equation (2) is solved by the predictor-corrector method, and the pressure equation is solved by the multigrid method to obtain intermediate variables at m+1/2 (see Watanabe et al. 2006). After the velocity is updated by eq. (2), eq. (3) is solved by the cubic interpolation polynomial (CIP) method (Yabe et al. 1991).

Level-set method (Sethian and Smereka 2003) is adopted to capture a free-surface. The level-set function ϕ, which indicates a distance to the nearest surface, is defined at computational grids near the surface. The reinitializing method proposed by Sussman and Fatemi (1999) is used to maintain the level-set function as a distance function. An unit normal vector on a surface $\mathbf{n}$ and surface curvature κ can be computed by

$$\mathbf{n} = \frac{\nabla\phi}{|\nabla\phi|}, \tag{4}$$

$$\kappa = \nabla \cdot \frac{\nabla\phi}{|\nabla\phi|}. \tag{5}$$

A dynamic FSBC appropriately imposed on a surface in the proposing technique will be explained in the following sections.

2.1 Free-surface boundary conditions

Normal and tangential components of the dynamic FSBC are expressed by

$$p = 2\tau\kappa + 2\mu\frac{\partial u_n}{\partial n}, \tag{6}$$

$$\mu\left(\frac{\partial u_n}{\partial t_1} + \frac{\partial u_{t_1}}{\partial n}\right) = 0,\ \mu\left(\frac{\partial u_n}{\partial t_2} + \frac{\partial u_{t_2}}{\partial n}\right) = 0, \tag{7}$$

where μ is the viscosity, and u_i is the fluid velocity in the x, y and z axes denoted by i= 1, 2 and 3, respectively. n and t_i (i = 1, 2) are the normal and tangential unit vectors of the free-surface and τ is the surface tension coefficient. Equation (6) represents a discontinuous jump of pressure across the surface due to the surface tension and viscosity and eq. (7) represents zero tangential shear conditions on the free-surface.

2.2 Numerical technique to impose FSBC

The zero tangential shear conditions (eq. (7)) are numerically achieved at the free-surface in a fixed Cartesian grid system on the basis of first-order extrapolations of velocity gradients from the inner fluid to the free-surface.

Assuming that the local velocity gradients at an arbitrary position ($\mathbf{x}_s + \boldsymbol{\xi}$) of inner fluid near the free-surface can be determined by the sum of the velocity gradients at the surface location ($\mathbf{x}_s$) and correction function f_{ij}:

$$\frac{\partial u_i(\mathbf{x}_s + \boldsymbol{\xi})}{\partial x_j} = \frac{\partial u_i^s(\mathbf{x}_s)}{\partial x_j} + f_{ij}(\boldsymbol{\xi}), \tag{8}$$

where $\mathbf{x}_s$ is the position vector on the surface and $\boldsymbol{\xi}$ is the relative position vector from $\mathbf{x}_s$. In our method, a first-order polynomial $f_{ij}(\boldsymbol{\xi}) = a_{ij}\xi_i$ is chosen as a correction function. The coefficient tensor a_{ij} is computed by the method of least squares for the zero shear conditions (eq. (7)) to which eq. (8) is substituted. In this way, appropriate surface velocity gradients $\partial u_i^s / \partial x_j$ and surface velocity u_i^s can be obtained by using the inner velocity near the surface.

In order to compute the advection term of the momentum equation (eq. (3)) in the fixed grid system, the fluid velocity needs to be extrapolated to empty grids. The local velocity on the outside of the surface is assumed to be described by keeping the first order of Taylor series for the velocity with respect to the surface location:

$$u_i(\boldsymbol{\xi}) = u_i^s + \frac{\partial u_i^s}{\partial x_j}\xi_j \tag{9}$$

The outer grid velocity can be extrapolated by using the surface velocity and its gradients that have been known through the above procedure. In this way, the zero shear conditions (eq. (7)) can be approximately satisfied at the surface.

The pressure jump condition (eq. (6)) is given as a boundary condition for the pressure equation.

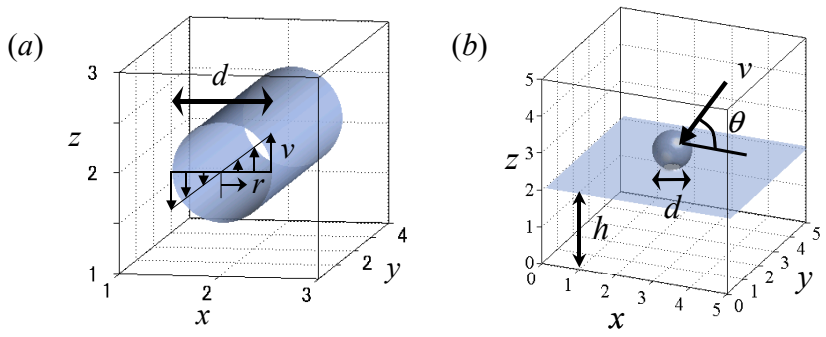

Figure 1 Computational domain for a rotating water cylinder in the numerical test (*a*). *d* is the cylinder diameter and *v* is the surface velocity. The droplet impacting at an angle θ onto the target water pool of the depth *h* (*b*). *d* is the droplet diameter and *v* is the impacting velocity.

3. COMPUTATIONAL CONDITIONS

3.1 Numerical test for "sold-body rotation"

In numerical tests for examining accuracies of our method, surface shears on a rotating water cylinder is investigated. Figure 1-(*a*) shows the computational domain for this test. The cylinder diameter *d* and axisymmetric linear distribution of fluid velocity in the cylinder ($v = ar$, a: constant, r: distance from the cylinder center) are given.

3.2 Impacting droplet

Figure 1-(*b*) shows the computational domain and impact condition for vertically and obliquely dropping droplet. A spherical droplet of the diameter *d* with the impacting velocity *v* at impacting angle θ is dropped onto the still water pool of the depth *h*. Periodic boundary and non-slip boundary conditions are given at the sidewalls and bottom of the computational domain.

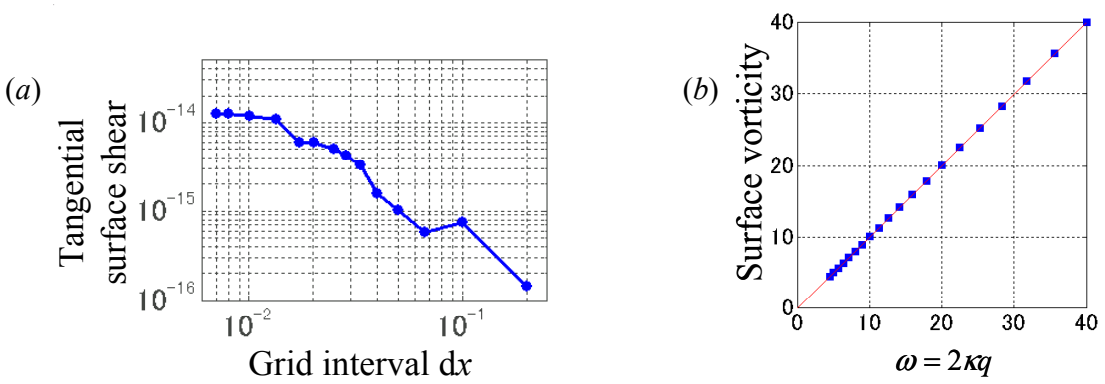

Figure 2 Computational error of the tangential surface shear in the rotating water cylinder (*a*), and comparison of the computed vorticity on the cylinder surface and the analytical solution (*b*).

4. NUMERICAL TESTS

4.1 Surface shear and vorticity on a rotating water cylinder

The numerical test of the "solid-body rotation" (Longuet-Higgins 1992) is carried out to confirm whether the tangential surface shear properly vanishes on the surface and to examine the numerical accuracies. The tangential surface shear and surface vorticity on a rotating water cylinder are computed using the present technique (see Fig. 1-(*a*)).

Figure 2-(*a*) shows the tangential shear on the cylinder surface, which should be zero, against the computational grid interval dx. The surface shear is found to be less than $O(10^{-13})$ for any computational grid interval, which is less than the machine precision and is therefore negligible.

Figure 2-(*b*) shows the computed surface vorticity and analytical solution $\omega = 2\kappa q$ on the cylinder surface, where ω is the tangential surface vorticity and q is the tangential surface velocity. Our results present very good agreements with the solutions, demonstrating a high level of accuracy of our method.

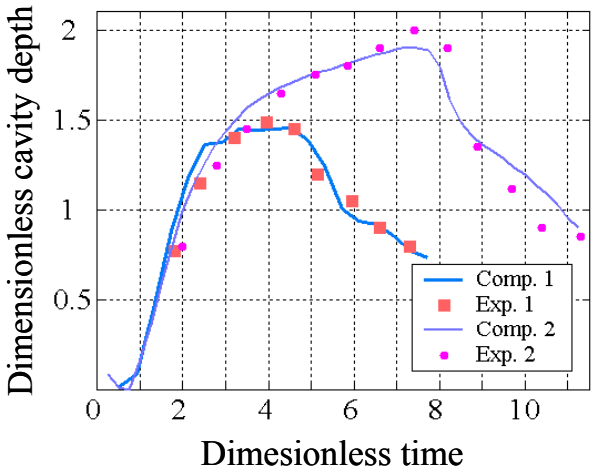

Figure 3 Dimensionless cavity depth against dimensionless time from the droplet impact. (1) v = 1.29 [ms^{-1}], d = 1.86 [mm]. (2) v = 1.61 [ms^{-1}], d = 2.09 [mm].

4.2 Droplet impacts

The local free-surface flow under impacting droplets is computed to compare the surface deformation with experimental measurements of Liow (2001). A droplet of which the diameter $d \approx 2$ [mm] is dropped onto a still water surface at the impacting velocity v (see Fig. 1-*b*). The computational grid interval dx was d/10.

Figure 3 shows the evolution of the cavity depth after the impact. The computational cavity depth was defined as a distance from a still water level to the deepest level of the cavity. There are good agreements in the computed cavity depths with the experimental results, demonstrating high capability of the present method for practical computations of free-surface flows.

5. COMPUTATIONAL RESULTS

The local surface deformation and vortex formation beneath the surface are significantly affected by the surface-vortex interactions (Sarpkaya 1996). A typical formation of a vortex ring under a

plunging droplet is also due to the surface-vortex interactions and the proposed method is applied to this problem for understanding the jet-induced vortex structure. A spherical droplet of which the diameter d = 0.1 [m] is dropped onto a still water at impacting velocity v = 1.0 [ms^{-1}] at two different impacting angles θ (see Fig. 1-(*b*)). The computational domain is a cube 5d on a side and the computational grid interval dx is d/20.

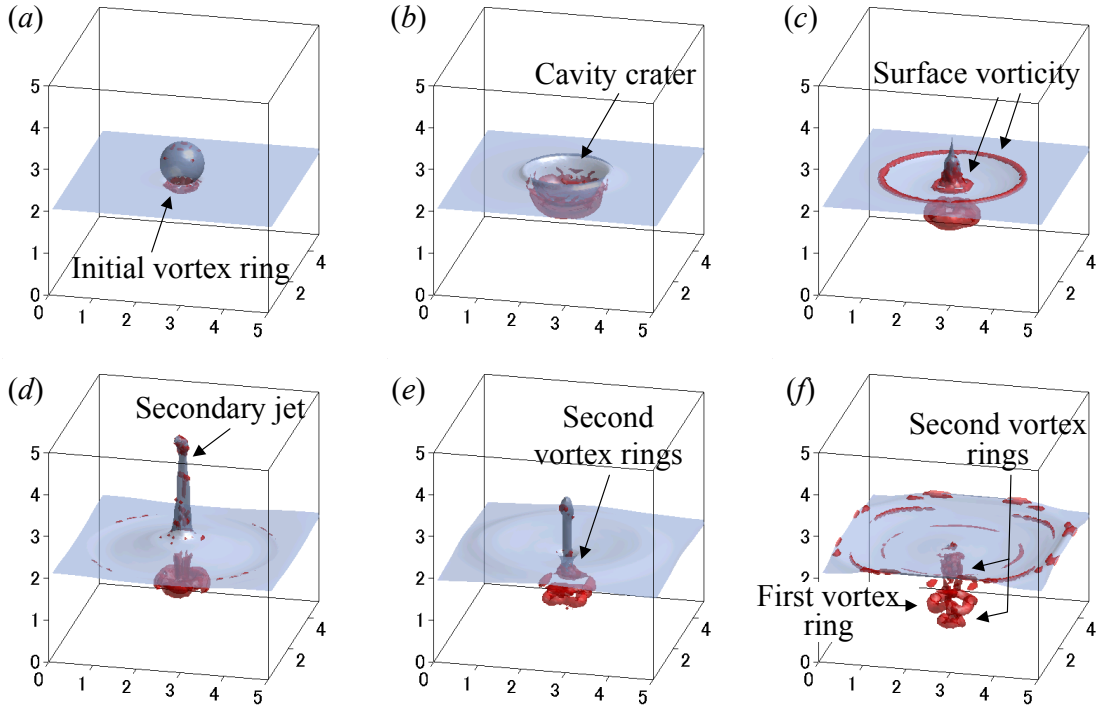

Figure 4 Evolution of the free-surface and vortex structure under the vertical impact of the droplet (d = 0.1 [m], v = 1.0 [m/s], $\theta = \pi/2$). (*a*) $t = 0.1d/v$, (*b*) $t = 1.2d/v$, (*c*) $t = 2.6d/v$, (*d*) $t = 4.3d/v$, (*e*) $t = 6.4d/v$, (*f*) $t = 7.8d/v$.

5.1 Vertical impact of a droplet

Figure 4 shows the evolution of the free-surface and vortex cores after the vertical impact ($\theta = \pi/2$). The vortex core is computed on the basis of λ_2-method (Jeong and Hussain 1995). The primary vortex ring is initiated at contacts between the droplet and target fluid (Fig. 4-(*a*)) since the vorticity must be induced on the curved surface. A cavity crater is formed by the impact, and the vortex ring is developed under the cavity bottom (Fig. 4-(*b*)). In Fig. 4-(*c*), the cavity bounces back due to the pressure gradient towards the center of the cavity, and then the vortex ring is ejected downwards from the cavity bottom. It is also seen that the surface vorticity is generated on a radically propagating cavity front and near the secondary jet projecting upward. The jet finally plunges again into water to produce another vortex ring (Fig. 4-(*e*)). The second vortex ring is rapidly displaced downward faster than the previous adjacent ring due to vortex-vortex interaction and pass through the previous vortex ring (Fig. 4-(*f*)).

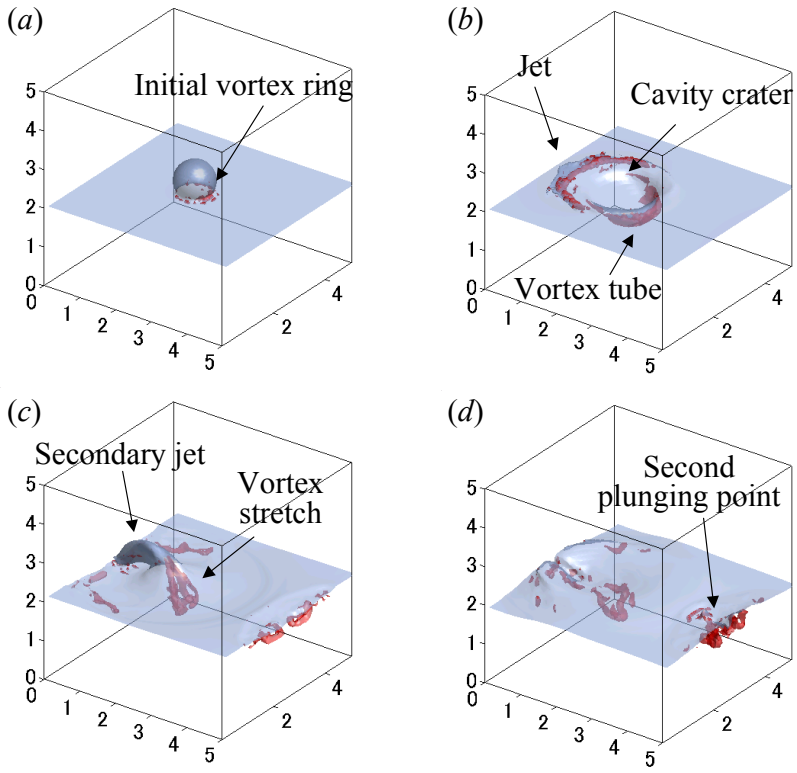

Figure 5 Evolution of the free-surface and vortex structure under the oblique impact of the droplet (d = 0.1 [m], v = 1.0 [m/s], $\theta = \pi/4$). (*a*) $t = 0.2d/v$, (*b*) $t = 1.3d/v$, (*c*) $t = 4.0d/v$, (*d*) $t = 6.2d/v$.

5.2 Oblique impact of a droplet

Figure 5 shows the evolving free-surface and vortex cores produced by the droplet impacting at $\theta = \pi/4$. More complicated flow field is formed in this case. A bore-like jet projects ahead of the crater and produces a radical vortex tube underneath (Fig. 5-(*b*)). The vortex initiated at the contacts between the droplet and receiving water surface (Fig. 5-(*a*)) develops beneath a rear part of the cavity for being the vortex tube (Fig. 5-(*b*)). This vortex tube is obliquely stretched and intensified within the secondary jet through the stretch-and-intensification process, resulting in a formation of three-dimensional vortex structure. After the secondary jet touches down onto the forward surface, another three-dimensional vortices appear at the plunging point (Fig. 5-(*d*)).

6. CONCLUSIONS

The numerical technique to impose FSBC in a fixed Cartesian grid system for local surface flows governed by the surface-vortex interactions was proposed. It is confirmed that the tangential FSBC can be satisfied at high accuracy and the surface flow under impacting droplet can be reproduced using the present technique. The numerical experiments about the plunging droplets were performed to investigate the evolution of the free-surface and vortex structure under the impacting droplets.

The proposed method to impose the tangential FSBC appropriately reproduces local vortex structures on a curved surface in plunging droplets. The surface vorticity generated at contacts between the droplet and water surface is developed underneath the surface of a cavity and is released from the cavity to displace downward. The surface vortices work as sources of the turbulence in free-surface flows.

It is also found that a structure of the vortices depends on an impacting angle of the plunging jet with respect to a target fluid surface. While an axisymmetric vortex ring is formed around the cavity and displaced downward in the case of the vertical drop impact, in the obliquely plunging case, a vortex ring is highly deformed within a secondary jet projecting obliquely upward due to strong stretches along the jet.

REFERENCES

Brocchini, M. and Peregrine, D. H. (2001) "The Dynamics of Strong Turbulence at Free Surfaces. Part 1. Description", Journal of Fluid Mech. Cambridge University Press, Vol. 449, pp.225-254.

Jeoung, J. and Hussain, F. (1995) "On the Identification of a Vortex", Journal of Fluid Mech. Cambridge University Press, Vol. 285, pp.69-94.

Liow, J. L. (2001) "Splash Formation by Spherical Drops", Journal of Fluid Mech. Cambridge University Press, Vol. 427, pp.73-105.

Longuet-Higgins, M. S. (1992) "Capillary Rollers and Bores", Journal of Fluid Mech. Cambridge University Press, Vol. 240, pp. 658-679.

Sarpkaya, T. (1996) "Vorticity, Free-Surface, and Surfactants", Ann. Rev. Fluid Mech. Annual Reviews, Vol. 28, pp. 83-128.

Sethian, J. A. and Smereka, P. (2003) "Level Set Method for Fluid Interfaces", Annu. Rev. Fluid Mech. Annual Reviews, Vol. 35, pp. 341-372.

Sussman, M. and Fatemi, E. (1999) "An Efficient, Interface-Preserving Level Set Redistancing Algorithm and Its Application to Interfacial Incompressible Fluid Flow", Journal of Scientific Computing, Springer Netherlands, Vol. 20, No. 4, pp. 1165-1191.

Watanabe, Y. and Saeki, H. (1999) "Three-Dimensional Large Eddy Simulation of Breaking Waves", Coastal Engineering Journal, World Scientific, Vol. 41, Nos. 3 & 4, pp. 281-301.

Watanabe, Y., Saeki, H., and Hosking, R. J. (2005) "Three-Dimensional Vortex Structure under Breaking Waves", Journal of Fluid Mech. Cambridge University Press, Vol. 545, pp. 291-328.

Yabe, T., Ishikawa, T., Wang, P. Y. and Aoki, T. (1991) "A Universal Solver for Hyperbolic Equations by Cubic-Polynomial Interpolation I. Two- and Three-Dimensional Solvers", Comp. Phys. Comm. Vol. 66, pp. 233-242.

Yakhot, V. and Orszag, S. A. (1986) "Renormarization Group Analysis of Turbulence. I. Basic Theory", Journal of Scientific Computing, Springer Netherlands, Vol. 1, No. 1, pp. 3-51.